In-situ Optical Emission Spectroscopy during SLM of 304L Stainless Steel

Cody S. Lough, Luis I. Escano, Minglei Qu, Christopher C. Smith, Robert G. Landers, Douglas A. Bristow, Lianyi Chen, Edward C. Kinzel

Department of Mechanical and Aerospace Engineering, Missouri University of Science and Technology, Rolla, MO 65409

Abstract

This paper demonstrates the potential of in-situ Optical Emission Spectroscopy (OES) to monitor the Selective Laser Melting (SLM) process. A spectrometer is split into the beam path of a home-built SLM system to collect visible light emitted from the melt pool and plume. The in-line configuration allows signal collection regardless of the laser scan location. The spectral data can be used to calculate the temperature of the vapor plume and correlated with the melt-pool size. The effects of varying the atmosphere and pressure on the OES signal are also explored. These results demonstrate that OES can provide useful feedback to the SLM process for process monitoring and part validation. The challenges implementing OES in-line on a commercial SLM platform are discussed. This work was funded by Honeywell Federal Manufacturing & Technologies under Contract No. DE-NA0002839 with the U.S. Department of Energy.

1. Introduction

Selective Laser Melting (SLM) is a powder-bed based additive manufacturing (AM) process in which 3-Dimensional parts are built layer-by-layer. One challenge in AM processes are that the temperature history varies with the geometry. Measuring local processing conditions is critical for part validation and provides opportunities for feedback-based control. While photodiodes provide some information about the state of the process, the spectral content of light emitted from the melt pool and plume gives potential insight into the temperature, chemistry and pressure surrounding of the melt pool.

Optical Emission Spectroscopy (OES) has been demonstrated with laser welding to provide information about the chemical species and calculate the temperature and electron density in the vapor plume [1-3]. The spectroscopic data has also been correlated with features in the welds such as the depth to width ratio. OES methods developed for laser welding have also been extended to monitor powder metal deposition Direct Energy Deposition (DED) blown-powder process. Song and Mazumder measured chromium emission in directed metal deposition and used line intensity ratios to calculate plasma temperatures and used emission signal to predict chromium composition real-time during processing with H13 tool steel [4]. Ya et al. demonstrated the ability to relate OES signals to clad quality in laser metal deposition [5]. Nassar et al. used OES as a process monitoring tool to correlate emission line-to-continuum ratios to lack of fusion defects during directed-energy deposition of Ti-6Al-4V [6].

Work performed and funded by The Department of Energy's Kansas City National Security Campus is operated and managed by Honeywell Federal Manufacturing & Technologies, LLC under contract number DE-NA0002839.

While OES has been used in blown-powder AM, there are limited reports of applying OES to powder bed based AM. Dunbar et al. mounted a spectrometer at a fixed location in a powder bed based 3DSystems Prox-200 build chamber and reported emission signal as a function of defocusing the process laser [7]. Dunbar and Nassar used photodiodes with band pass filters focused off axis in the build chamber to monitor the chromium emission line to continuum ratio during processing of Inconel 718 with a 3DSystems Prox-200 powder bed AM system [8].

The galvo-scanner steered laser beam and moving melt pool in the global reference frame complicates implementation of OES for the SLM process. Inserting the spectrometer optics into the beam path allows the collection volume to also be guided by the galvo-scanner. Although the solid-angle is limited, the approach still allows species and plume temperatures to be determined. This paper demonstrates OES of the SLM process with 304L stainless steel.

2. Experimental Approach

Experiments to evaluate OES of SLM were completed using a home-built SLM system and an Andor Technology SR-750 spectrometer. The SLM system used an IPG Photonics YLR-500 continuous wave fiber laser (λ = 1070 nm) with an IPG D30 collimator. The *x-y* position of the laser beam was controlled by a SCANLAB hurrySCAN and the laser was focused by a 340 mm focal length *f-θ* lens (measured $1/e^2$ beam diameter of 145 μm). Data reported in the following section was collected using a 600 l/mm diffraction grating installed in the spectrograph and an Andor Technology iStar 734 series ICCD. The spectrometer was coupled to the SLM system as illustrated in Fig. 1 using a DMLP Dichroic mirror (Thorlabs).

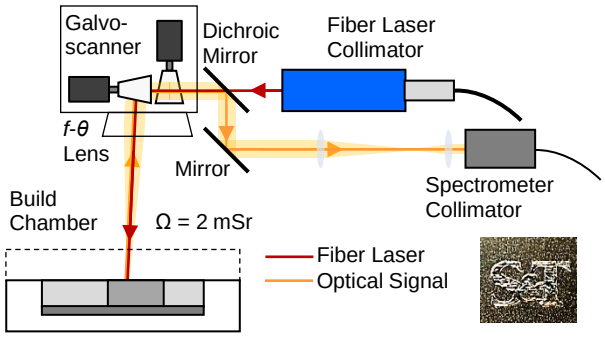

FIG 1: Schematic of SLM system optical components with spectrometer inserted into the beam path.

Relative intensities for optical emission lines are described by Eq. 1 [4]:

$$I_{mn} \propto N_m \cdot A_{mn} \cdot h \cdot \nu_{mn} \tag{1}$$

where I_{mn} is the intensity, N_m is the upper state population, A_{mn} is the transition probability, h is the Planck constant, and ν_{nm} is the frequency. Emission lines detected during SLM of 304L in this work correspond to neutral chromium and iron (determined species from NIST database). Figure 2 contains representative emission signal measured during laser melting a 304L stainless steel

powder bed with a laser power of 300 W and scan speed of 675 mm/s. In Fig. 2, both wavelength ranges investigated contain strong chromium emission lines and weaker iron lines.

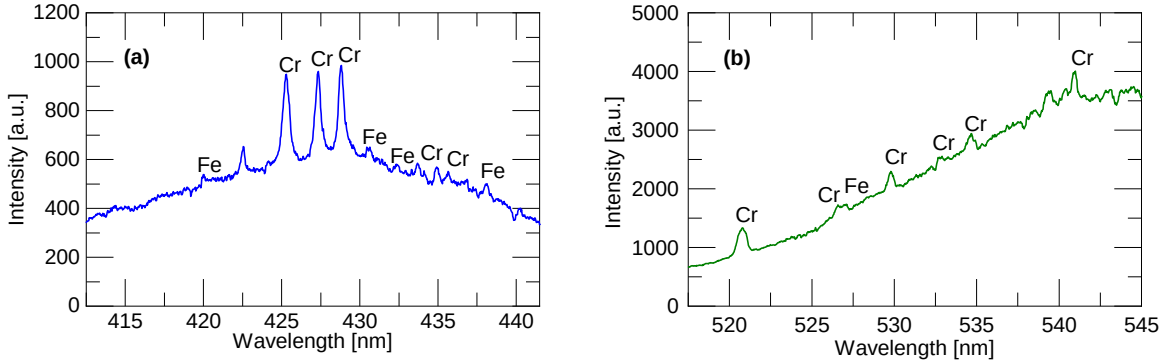

FIG 2: Average optical emission signal collected during processing powder 304L in argon build chamber atmosphere.

Figure 3 is an example of using OES signals to differentiate materials. The signals were collected during laser melting of solid plain carbon steel and solid 304 stainless steel samples with 300 W. Figure 3 shows both the plain carbon and stainless steel samples contain emission lines for iron and manganese. The signals in Figs. 2 and 3 give important information about the composition of the material during processing. The species identified in the vapor plume through OES should be consistent for a particular material. This means OES can be used to flag contaminated powder beds if unexpected emission lines are present in the signal.

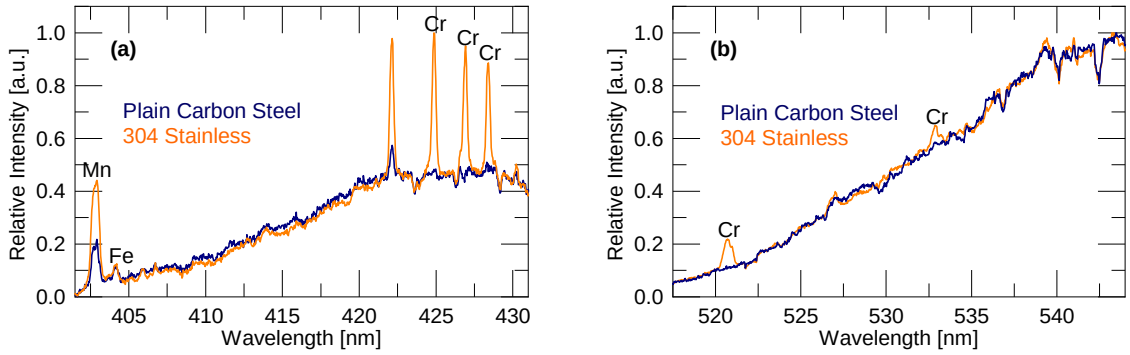

FIG 3: Differentiation of plain carbon steel and stainless steel through optical emission signals.

3. Results and Discussion

In addition to differentiation of materials during processing, OES can also be used to determine plume temperatures. Emission signals reported in the following figures are time series data averaged over laser melting 5×5 mm^2 areas of a 50 µm thick 304L stainless steel powder layer. Single layer samples were produced by processing the powder bed with varied laser powers and build chamber conditions (atmosphere and pressure). As shown in Fig. 2, the average signals

generated over a layer contained an incandescent background with optical emission signals superimposed. The OES data for this section was processed by excluding the optical emission lines to fit the background to a fourth-order polynomial. This fit was then subtracted from the average data including optical emission signals to remove effects of the incandescent background. The processed OES signals were then used to calculate the plume temperature and correlated with sample melt pool size.

Figure 4 (a) is the average optical emission spectra for 304L as a function of laser power collected during processing in an argon atmosphere. Assuming local thermodynamic equilibrium, plume temperatures can be calculated by comparing the intensities of two emission lines of the same species with $E_2 - E_1 > k \cdot T$. Temperature is calculated with OES data by using Eq. 2 [9]:

$$T = \frac{(E_2 - E_1)}{k \cdot \ln\left(\frac{I_1 \cdot A_2 \cdot g_2 \cdot \lambda_1}{I_2 \cdot A_1 \cdot g_1 \cdot \lambda_2}\right)} \tag{2}$$

where T is the temperature, E is the energy, k is the Boltzmann constant, I is emission line intensity, g is the statistical weight, and λ is the wavelength. The chromium emission lines at λ_1 = 529.827 nm and λ_2 = 532.834 nm satisfy all conditions and have previously been used in literature to calculate the plume temperature [5]. The intensities (I_1 and I_2) for λ_1 and λ_2 were determined as the intensity above background using the method described in [10]. Figure 4 (b) is the average plume temperature for processing 304L in an argon atmosphere with varied laser power.

Table 1: Constants for selected chromium lines used to calculate the plume temperature.

λ [nm]	A_{mn} [s^{-1}]	g_m	E_m [cm^{-1}]
529.827	3,300,000	5	26,797
532.834	62,000,000	11	42,263

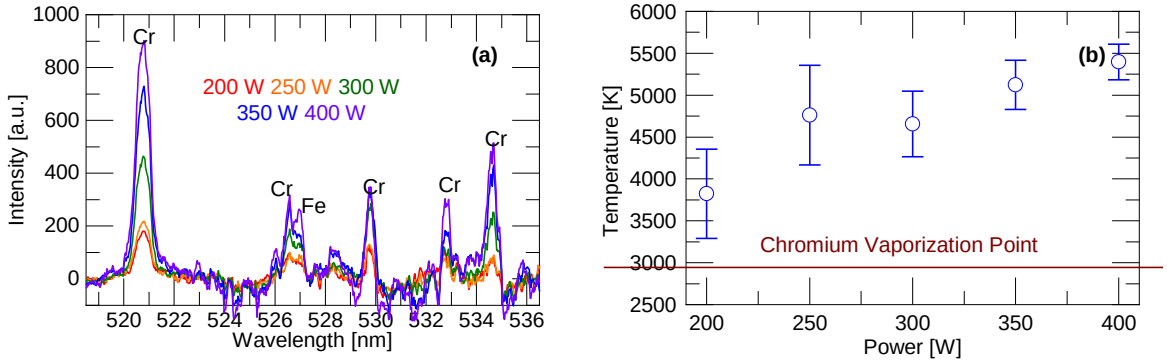

FIG 4: (a) Average optical emission spectra and (b) plume temperatures of 304L stainless steel for varied laser power.

In Fig. 4, the overall intensities of emission lines increase with laser power. The increased emission signal with laser power directly correlates to higher average plume temperatures during SLM of 304L.

In addition to varying with power, OES signals also change with build chamber atmosphere type and pressure. Figure 5 (a) is the average OES signal for processing 304L in air, argon, nitrogen, and low vacuum. The optical emission signal for air is much stronger than the other atmospheres. This could be due to increased material vaporization, which would be reflected in a keyhole mode like appearance of the melt pool. However, micrographs of the melt pool cross-sections (Fig 5 (d-g)) show conduction mode melting dominates regardless of chamber atmosphere. The increased OES signal strength for air could also be explained due to oxidation of the vaporized chromium and iron. The exothermic oxidation process adds heat to the plume increasing the temperature and resulting signal measured through OES [10]. The OES signals for processing in argon, nitrogen, and low vacuum are not amplified from the oxidation process.

Figure 5 (b) shows the dependence of optical emission signal on chamber pressure. OES data was collected while increasing the pressure of an argon atmosphere. The intensity of emission lines increases from low vacuum to above atmospheric pressure (0.2 to 800 Torr). The weaker optical emission signals measured near vacuum are possibly due to lower excitation efficiency because of less energy transferring collisions. Figure 5 (c) is the intensity of chromium emission λ=520.6 nm as a function of chamber pressure and also shows the dependence of layer surface quality for selected pressures (100, 400, and 700 Torr). Lower chamber pressures resulted in better surface finishes when compared to layers processed with higher pressure. This means the layers with higher surface finish quality correspond to weaker intensities of optical emission signals.

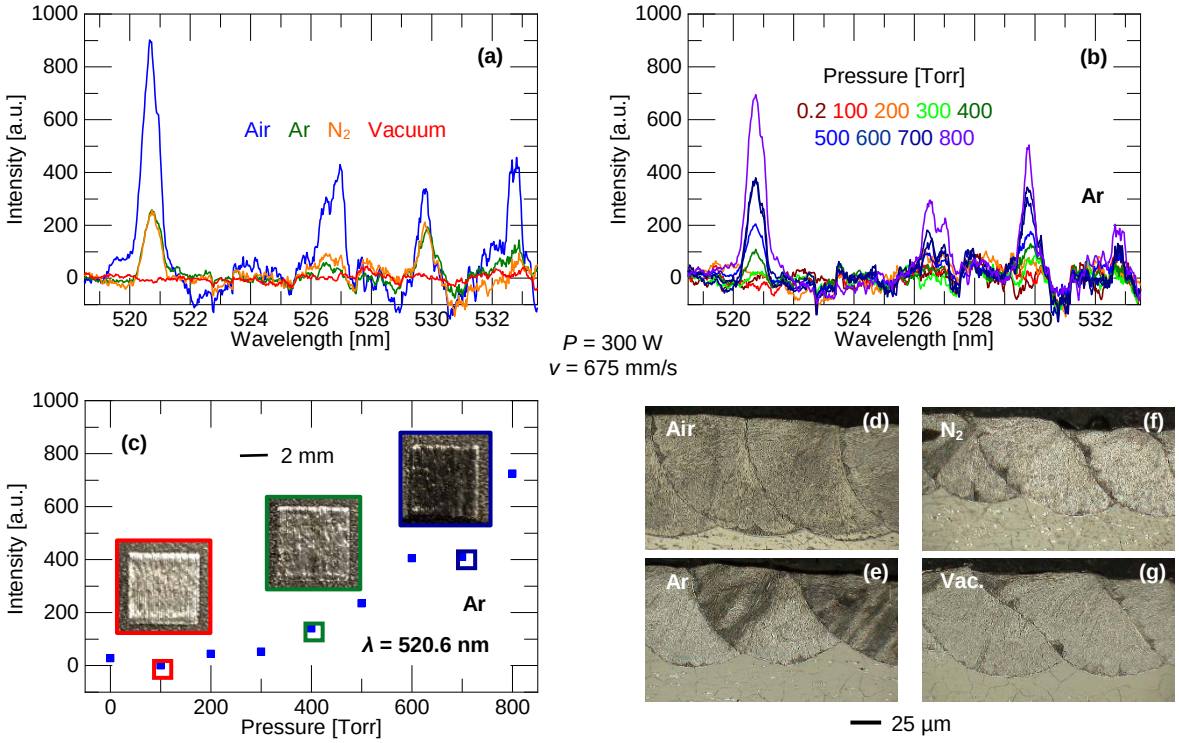

FIG 5: OES signal collected during SLM processing with different chamber atmospheres and pressures and micrographs of 304L stainless steel single layers.

Figure 6 is the correlation of the average plume temperatures determined by OES to the average melt pool size across single layer samples processed with varied laser power. Larger plume temperatures directly correlate to larger melt pools. Since OES data relates to sample properties, signals can potentially be used as feedback for control of SLM. This has been demonstrated in laser welding where the plume temperature determined by OES was used as feedback to control the penetration depth of the weld [11]. Similar OES feedback methods can be applied to SLM for layer-to-layer and point-to-point control.

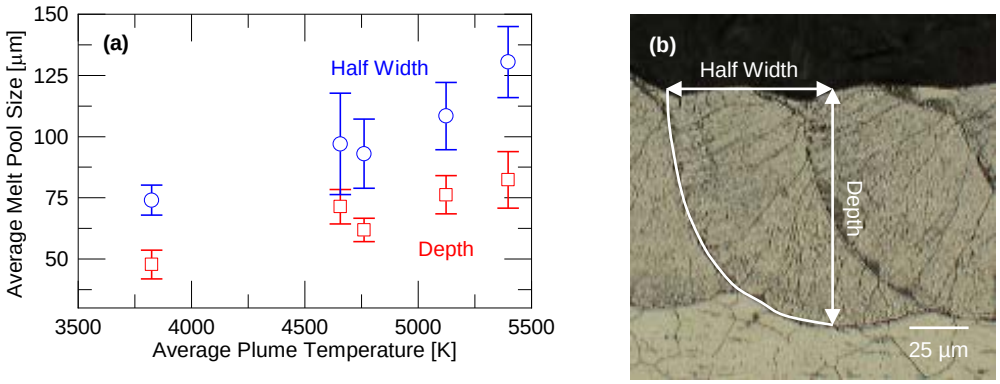

FIG 6: Correlation of melt pool size to average plume temperatures during single layer processing.

4. Challenges Implementing OES with Commercial System

The results in the previous sections show the potential value of using OES to monitor the SLM process based on results from a home-built system used for fundamental research and manufacturing of small scale samples. Implementing OES on a commercial system will allow an investigation of OES signals with correlation to engineering properties determined from larger scale samples. As a part of the first steps to accomplish this, an optical configuration similar to the schematic in Fig. 1 was applied to insert the spectrometer into the beam path of a Renishaw AM250. Figure 7 is an image of the spectrometer optics in-line on the AM250.

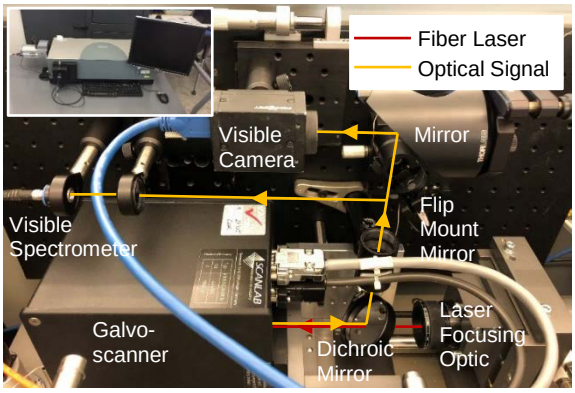

FIG 7: Image of experimental setup for inserting spectrometer optics into laser beam path of Renishaw AM250

The experimental setup in Fig. 7 was used in a preliminary investigation to identify challenges in performing OES with the spectrometer optics inserted into the beam path on the AM250. Figure 8 (a) contains the average optical emission signals collected during processing a 10 by 10 mm^2 area of a 50 µm thick powder layer of 304L stainless steel in argon. There are no apparent emission lines in Fig. 8 (a). This is due to low transmission of the AM250 galvo-scanner optics from 400 nm to 530 nm. However, it is known from Fig. 5 (a) optical emission signals are stronger for processing in air. The Renishaw AM250 process laser was used to scan and melt solid 304L in air to observe if optical emission signals can be detected. Figure 8 (b) is the successful measurement of chromium emission during laser melting of solid 304L in air with the spectrometer optics inserted into the Renishaw beam path.

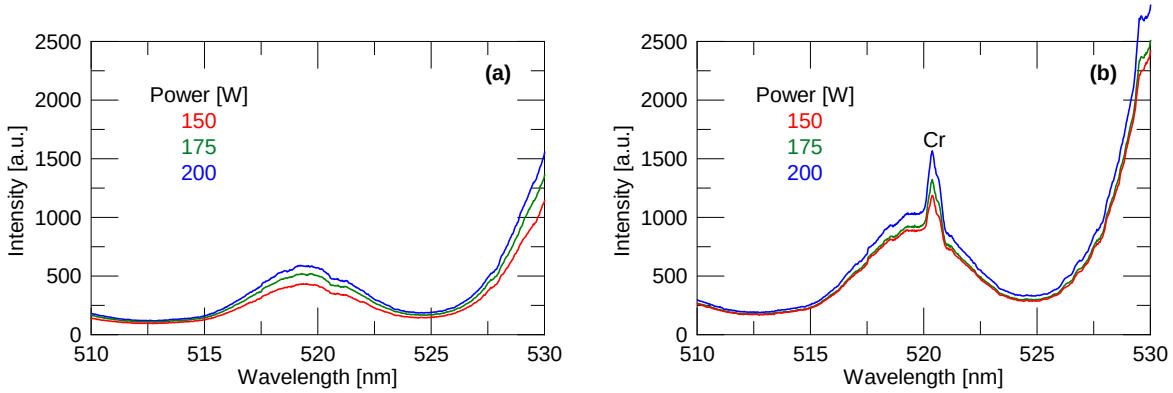

FIG 8: Signals collected during (a) processing powder 304L in an Argon atmosphere and (b) laser melting solid 304L in air with Renishaw AM250.

Figure 9 contains OES signals for two wavelength ranges measured during further investigation with laser melting solid 304L in air with the AM250 process laser (200 W). There are strong neutral chromium and iron signals present in Fig. 9 and the results are comparable to the signals in Fig. 2 obtained during SLM of powder 304L in argon with the home-built system.

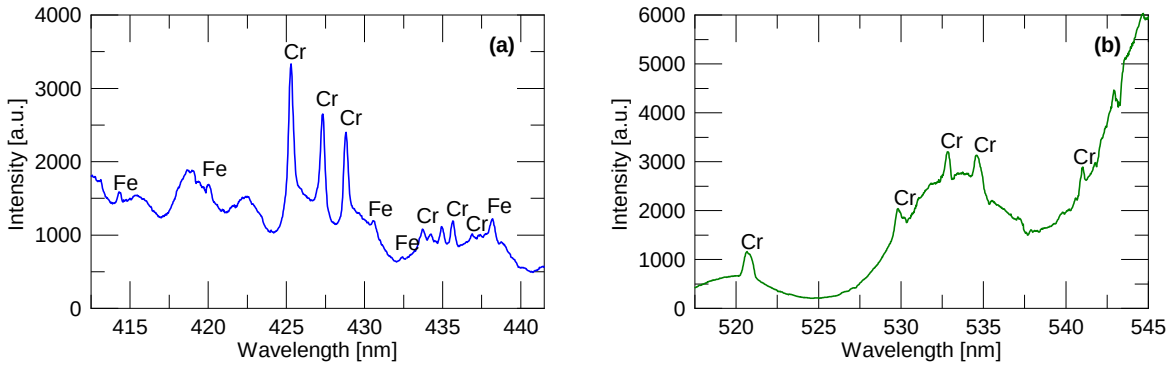

FIG 9: OES signal collected during laser melting solid 304L in air with Renishaw AM250.

Figures 8 and 9 show the methods used to insert the spectrometer optics into the laser beam path on the home-built SLM system can be expanded to a commercial platform. However, the current transmission of the Renishaw AM250 galvo-scanner optics and spectrometer optical elements attenuates the emission signal during processing powder 304L with nominal conditions. The challenge of low transmission will be addressed in future work in order to correlate optical emission data with engineering properties of specimens manufactured with the Renishaw AM250.

5. Summary and Conclusions

This paper demonstrated measurement of the SLM plume using in-situ OES. The temperature of the plume generated during SLM was determined by comparing ratios of optical emission signal intensities. The calculated plume temperatures correlate well with the melt pool

size. The OES results in this paper also show the dependence of SLM on build chamber atmosphere type and pressure, with higher chamber pressures resulting in stronger intensities of optical emission signals. The correlation of signals measured with OES to sample properties leads to the potential for feedback control with faster spectrometer data. Future work will involve expanding the process windows to include scan speeds and building multi-layer parts with a commercial SLM system to demonstrate the correlation of engineering properties to information determined by using OES.

6. Acknowledgement

This work was funded by Honeywell Federal Manufacturing & Technologies under Contract No. DE-NA0002839 with the U.S. Department of Energy. The United States Government retains and the publisher, by accepting the article for publication, acknowledges that the United States Government retains a nonexclusive, paid up, irrevocable, world-wide license to publish or reproduce the published form of this manuscript, or allow others to do so, for the United States Government purposes.

7. References

[1] Collur M, Debroy T. Emission Spectroscopy of Plasma During Laser Welding of AISI 201 Stainless Steel. Metallurgical Transactions B. 1989; 20B:277-86.

[2] Szymanski Z, Kurzyna J, Kalita W. The spectroscopy of the plasma plume induced during laser welding of stainless steel and titanium. Journal of Physics D: Applied Physics. 1997; 30:3153-62.

[3] Kawahito Y, Matsumoto N, Mizutani M, Katayama S. Characterization of plasma induced during high power fiber laser welding of stainless steel. Science and Technology of Welding and Joining. 2008; 13:744-8.

[4] Song L, Mazumder J. Real Time Cr Measurement Using Optical Emission Spectroscopy During Direct Metal Deposition Process. IEEE Sensors Journal. 2012; 12:958-64.

[5] Ya W, Konuk A, Aarts R, Pathiraj B, Veld B. Spectroscopic monitoring of metallic bonding in laser metal deposition. Journal of Materials Processing Technology. 2015; 220:276-84.

[6] Nassar A, Spurgeon T, Reutzel E. Sensing defects during directed-energy additive manufacturing of metal parts using optical emissions spectroscopy. Solid Freeform Fabrication Symposium; 2014.

[7] Dunbar A, Nassar A, Reutzel E, Blecher L. A real-time communication architecture for metal powder bed fusion additive manufacturing. Solid Freeform Fabrication Symposium; 2016.

[8] Dunbar A, Nassar A. Assessment of optical emission analysis for in- process monitoring of powder bed fusion additive manufacturing. Virtual and Physical Prototyping. 2018; 13:14-9.

[9] Ancona A, Spagnolo V, Lugara P, Ferrara M. Optical sensor for real-time monitoring of CO_2 laser welding process. Applied Optics. 2001; 40:6019-25.

[10] Shin J, Mazumder J. Composition monitoring using plasma diagnostics during direct metal deposition (DMD) process. Optics and Laser Technology. 2018; 106:40-6.

[11] Sibillano T, Rizzi D, Mezzapesa F, Lugara P, Konuk A, Aarts R, Veld B, Anoca A. Closed Loop Control of Penetration Depth during CO_2 Laser Lap Welding Process. Sensors. 2012; 12:11077-90.